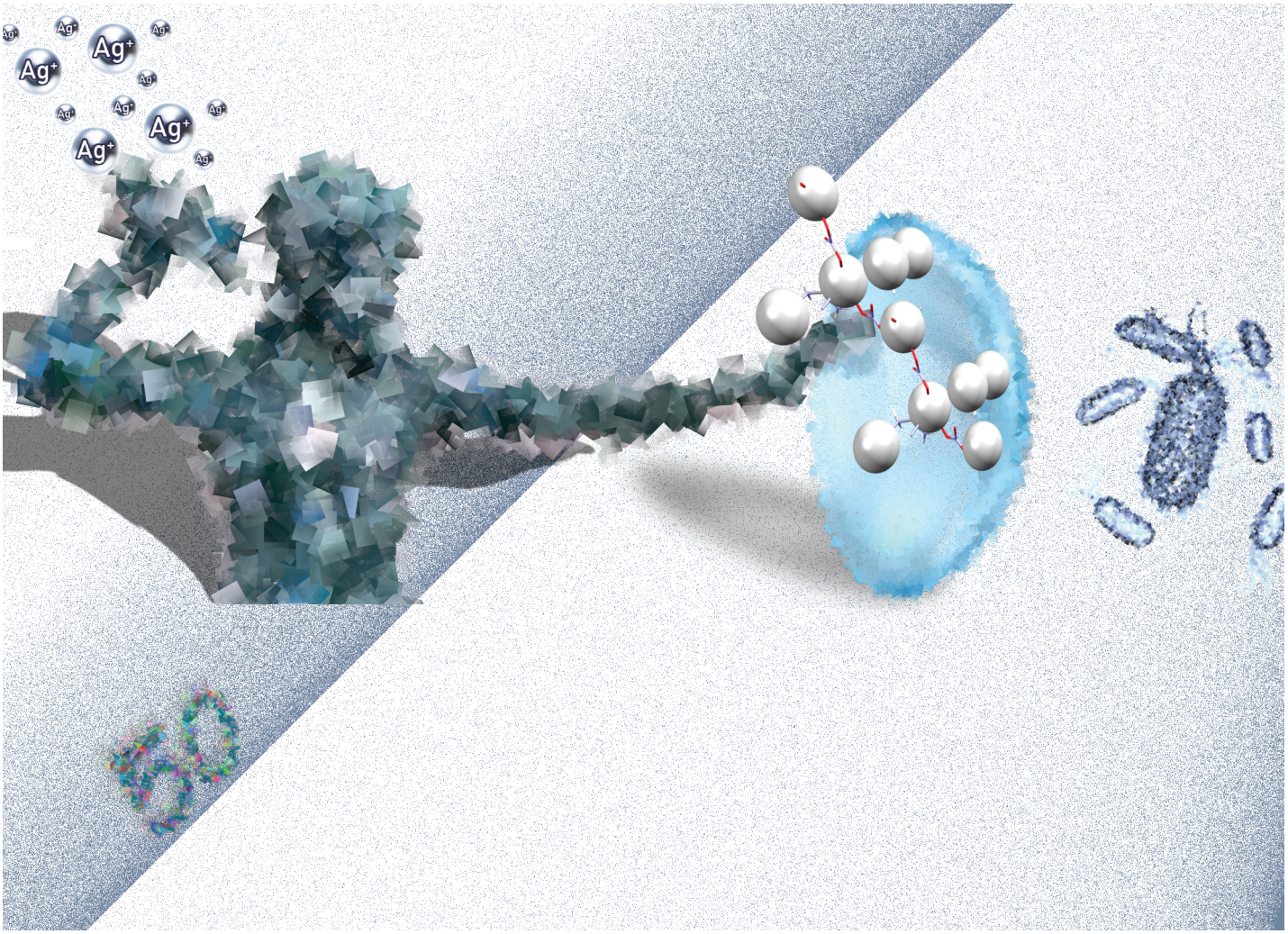

Showcasing research from the Biological Inorganic Chemistry Laboratory (Professor Sotiris K. Hadjikakou), of the Department of Chemistry in the University of Ioannina, Greece.

Hydrogels containing water soluble conjugates of silver(I) ions with amino acids, metabolites or natural products for non infectious contact lenses

The poor handling and hygiene practices of contact lenses are the key reasons for the frequent contamination of them, which is responsible for developing ocular complications. Thus, for the development of biomaterials, combined to antimicrobial agents for contact lenses the water-soluble silver(I) covalent polymers of Glycine (GlyH), Urea (U) and the Salicylic acid ($SalH_2$) were dispersed in polymeric hydrogels using, hydroxyethyl-methacrylate (HEMA) to form the biomaterials pHEMA@AGGLY-2, pHEMA@AGU-2, and pHEMA@AGSAL-2.

As featured in:

See C. N. Banti, S. K. Hadjikakou *et al.*, *Dalton Trans.*, 2021, **50**, 13712.

ROYAL SOCIETY OF CHEMISTRY

rsc.li/dalton

Registered charity number: 207890

Dalton Transactions

ROYAL SOCIETY OF CHEMISTRY

PAPER

View Article Online
View Journal | View Issue

Cite this: *Dalton Trans.*, 2021, **50**, 13712

Hydrogels containing water soluble conjugates of silver(I) ions with amino acids, metabolites or natural products for non infectious contact lenses†

C. N. Banti, *[a] M. Kapetana,[a] C. Papachristodoulou,[b] C. P. Raptopoulou,[c] V. Psycharis, [c] P. Zoumpoulakis,[d] T. Mavromoustakos[e] and S. K. Hadjikakou *[a,f]

The poor handling and hygiene practices of contact lenses are the key reasons for their frequent contamination, and are responsible for developing ocular complications, such as microbial keratitis (MK). Thus there is a strong demand for the development of biomaterials of which contact lenses are made, combined with antimicrobial agents. For this purpose, the known water soluble silver(I) covalent polymers of glycine (GlyH), urea (U) and the salicylic acid ($SalH_2$) of formulae $[Ag_3(Gly)_2NO_3]_n$ (**AGGLY**), $[Ag(U)NO_3]_n$ (**AGU**), and dimeric $[Ag(salH)]_2$ (**AGSAL**) were used. Water solutions of **AGGLY**, **AGU** and **AGSAL** were dispersed in polymeric hydrogels using hydroxyethyl-methacrylate (HEMA) to form the biomaterials **pHEMA@AGGLY-2**, **pHEMA@AGU-2**, and **pHEMA@AGSAL-2**. The biomaterials were characterized by X-ray fluorescence (XRF) spectroscopy, thermogravimetric differential thermal analysis (TG-DTA), differential scanning calorimetry (DTG/DSC), attenuated total reflection spectroscopy (FT-IR-ATR) and single crystal diffraction analysis. The antibacterial activity of **AGGLY**, **AGU**, **AGSAL**, **pHEMA@AGGLY-2**, **pHEMA@AGU-2** and **pHEMA@AGSAL-2** was evaluated against the Gram negative species *Pseudomonas aeruginosa* (*P. aeruginosa*) and Gram positive ones *Staphylococcus epidermidis* (*S. epidermidis*) and *Staphylococcus aureus* (*S. aureus*), which mainly colonize in contact lenses. The *in vitro* toxicity of the biomaterials and their ingredients was evaluated against normal human corneal epithelial cells (HCECs) whereas the *in vitro* genotoxicity was evaluated by the micronucleus (MN) assay in HCECs. The *Artemia salina* and *Allium cepa* models were applied for the evaluation of *in vivo* toxicity and genotoxicity of the materials. Following our studies, the new biomaterials **pHEMA@AGGLY-2**, **pHEMA@AGU-2**, and **pHEMA@AGSAL-2** are suggested as efficient candidates for the development of antimicrobial contact lenses.

Received 28th June 2021,
Accepted 11th August 2021

DOI: 10.1039/d1dt02158c

rsc.li/dalton

Introduction

The use of soft contact lenses is a popular method for correcting eye refractive errors.[1] Their poor handling and hygiene practices are the key reasons for their frequent contamination, which can lead to microbial keratitis (MK).[2] MK is an infection of the cornea, which occurs at a rate of approximately 3 per 10 000 wearers per year.[3,4] Despite the rare occurrences of MK development, the high number of soft contact lens wearers (45 million in the United States) leads to thousands of cases, annually.[5,6] A strategy for manufacturing next generation soft contact lenses involves the use of novel active biomaterials which control microbial colonisation and thus the incidence of MK.[3] Attempts towards this direction have been made either by loading an antimicrobial agent in the hydrogels, of which contact lenses are made, or by functionalizing the surface of contact lenses with an antimicrobial component.[2]

Silver(I), on the other hand, exhibits a broad spectrum of antimicrobial activity against both Gram-positive and Gram-negative bacteria.[1] Currently, silver nitrate solution (1–2%) is extensively used for curing neonatal conjunctivitis.[4] Moreover, silver-impregnated contact lens cases, (MicroBlock®) have

[a]*Inorganic and Analytical Chemistry, Department of Chemistry, University of Ioannina, 45110 Ioannina, Greece. E-mail: cbanti@uoi.gr, shadjika@uoi.gr*
[b]*Department of Physics, University of Ioannina, Greece*
[c]*NCSR "Demokritos", Institute of Nanoscience and Nanotechnology, A. Paraskevi, Attikis, Greece*
[d]*Laboratory of Chemistry, Analysis & Design of Food Processes, Department of Food Science and Technology, University of West Attica, Greece*
[e]*Organic Chemistry Laboratory, Department of Chemistry, University of Athens, Greece*
[f]*University Research Center of Ioannina (URCI), Institute of Materials Science and Computing, Ioannina, Greece*

†Electronic supplementary information (ESI) available. CCDC 2089744. For ESI and crystallographic data in CIF or other electronic format see DOI: 10.1039/d1dt02158c

been on the market in the United Kingdom since 2004, and were approved for use in the United States in 2005.[1] Upon adding the contact lens solution to the MicroBlock® (or ProGuard) case, silver ions at concentrations of approximately 10 μg L^{-1} are released into the solution for about one month protecting the lenses from microbial colonaization.[4] Generally, a slow release of silver ions maintains the antimicrobial activity in a macromolecular environment by inhibiting the growth of microorganisms.[7] Therefore, the development of biomaterials of which contact lenses are made combined with silver based antimicrobial agents is a research, technological and financial issue. For this purpose, two strategies have been developed by our group. One involves the use of silver nanoparticles using extracts from natural products as combined reducing and capping agents.[8] The second one involves the use of small molecules which act as antimicrobial agents as well.[5,8–10] However, it is of interest to study whether small molecules which are natural product ingredients could lead to biocompatible, non-toxic agent formation and thus to the formation of effective antimicrobial materials. In the course of our studies on the development of new antimicrobial agents[5,8,9,11–21] and their non-infectious contact lenses the novel biomaterials **pHEMA@AGGLY-2**, **pHEMA@AGU-2**, and **pHEMA@AGSAL-2** were synthesised by dispersion in polymeric poly(2-hydroxyethyl methacrylate) (pHEMA) of the known water soluble silver(I) covalent polymers $[Ag_3(Gly)_2NO_3]_n$ (**AGGLY**), $[Ag(U)NO_3]_n$ (**AGU**), and dimeric $[Ag(salH)]_2$ (**AGSAL**) (GlyH = glycine, U = urea and $SalH_2$ = salicylic acid). The biomaterials were characterized by XRF, TG-DTA, DTG/DSC and FT-IR-ATR analytical techniques. The prepared materials were evaluated for their antibacterial activity against the Gram negative species *P. aeruginosa* and Gram positive ones *S. epidermidis* and *S. aureus* which are abundant in microbial keratitis. The *in vitro* and *in vivo* toxicity of the biomaterials was tested against HCECs, by the MN assay, using *Artemia salina* and *Allium cepa* models.

Results and discussion

General aspects

The known silver(I) covalent polymers **AGGLY**, **AGU** and dimeric **AGSAL** were readily obtained by reacting $AgNO_3$ with GlyH, U or $SalH_2$ (Scheme 1).[22–24] Briefly, $AgNO_3$ reacts with the potassium salts of GlyH or $salH_2$ in dd water in 2 : 3 (**AGGLY**) and 1 : 1 (**AGSAL**) molar ratios (Scheme 1). The white precipitates were crystallized from DMSO solutions to form colourless crystals of the named compounds of formulae $[Ag_3(Gly)_2NO_3]_n$ (**AGGLY**) or $[Ag(salH)]_2$ (**AGSAL**).[13,22–24] Colourless crystals of $[Ag(U)NO_3]_n$ (**AGU**) were grown from the methanol/acetonitrile solution of $AgNO_3$ and U (1 : 1 molar ratio). **AGGLY**, **AGU** and **AGSAL** are soluble in H_2O and DMSO.

The formation of **AGGLY**, **AGU** and **AGSAL** was verified from their physical constants (m.p. and ATR-FT-IR).[13,22–24] The vibrational spectra of **AGGLY** and **AGSAL** (Fig. S1 and S2†) are identical to those of the published ones.[13,22–24] The ATR-FT-IR spectrum of **AGU** shows vibration bands at 1674 and 3354 cm^{-1}, which are attributed to ν(C=O) and ν(N–H), respectively (Fig. S3†). The corresponding vibration bands in the IR spectrum of urea are observed at 1690 and 3355 cm^{-1} (Fig. S4†).[25,26] The ν(C–N) vibration band is observed at 1465 cm^{-1} in the spectrum of **AGU**.[25] The vibration band at 1384 cm^{-1} is assigned to the NO_3 group.[25]

The crystal structures of both **AGGLY** and **AGSAL** are already refined by single crystal X-ray crystallography and they are reported elsewhere (Fig. 1 and 2).[13,22–24] Their structures are briefly described here: **AGGLY** shows a polymeric 3D structure (Fig. 1).[22] There are three symmetry independent Ag(I) cations, two symmetry independent deprotonated glycine ligands, one nitrate anion and one water solvent molecule in a lattice site with half occupancy in the asymmetric unit of the unit cell. Thus, the charge balanced stoichiometric formula of **AGGLY** is $\{[Ag_3(Gly)_2NO_3]\cdot 0.5H_2O\}$ (Fig. 1).[22] The architecture of the structure is based on the centrosymmetric $Ag_6(NO_3)_2^{4-}$ unit presented in Fig. 1.[22] **AGSAL** is dimeric (Fig. 2). Two silver atoms are bridged together by two carboxylic groups from two $SalH_2$ ligands (Fig. 2).[13,23] Strong Ag···Ag interactions (2.856 Å) are established due to argentophilicity, which leads to metalloaromaticity in the 5-member rings. This adds further stabilization to the assembly.

The structure of **AGU** has been studied previously at room temperature and in the present discussion an emphasis is given in the packing and the hydrogen bond interactions.[24] **AGU** crystallized in $P2_1/n$ with a = 6.2509(1), b = 16.8667(4), c = 10.2467(3) Å, 102.191(1)°, V = 1055.97(4) $Å^3$, Z = 4, R = 2.31%, while the reported one crystallized in $P2_1/n$ with a = 6.314(4), b = 16.886(4), c = 10.270(8) Å, β = 104.80(5)°, V = 1068(l) A^3, Z = 4, R = 7.7% (ref. 24). Selected bond distances and angles are listed in Fig. 3, while extensive quoting is listed in Table AGU-1, ESI.† A detailed description of the supramolecular assembly is provided in the ESI (see the ESI†). The building block of the entire **AGU** is shown in Fig. 3A. The compound is polymeric. The chains consist of $[–Ag(U)–NO_3–]_n$ units. The secondary $N_{(urea)}$–Ag bonds link different chains (Fig. 3). The geometry around silver is distorted trigonal bi-pyramidal. Three oxygen atoms from two NO_3^- groups and one from urea coordinate to the metal centre, while the coordination sphere is completed by two N atoms of amide groups originating from two different ureas.

Agent loading in pHEMA

Aqua solutions of **AGGLY**, **AGU** and **AGSAL** (2 mM) were dispersed in pHEMA (Scheme 2) during the polymerization procedure towards the formation of biomaterials **pHEMA@AGGLY-2**, **pHEMA@AGU-2**, and **pHEMA@AGSAL-2**. The dispersion of **AGGLY**, **AGU** and **AGSAL** in pHEMA was qualitatively verified by XRF, UV solid, TG-DTA and DTG/DSC analyses.

X-ray fluorescence spectroscopy

The XRF spectra of **pHEMA@AGGLY-2**, **pHEMA@AGU-2** and **pHEMA@AGSAL-2** confirm the presence of Ag. Moreover, the

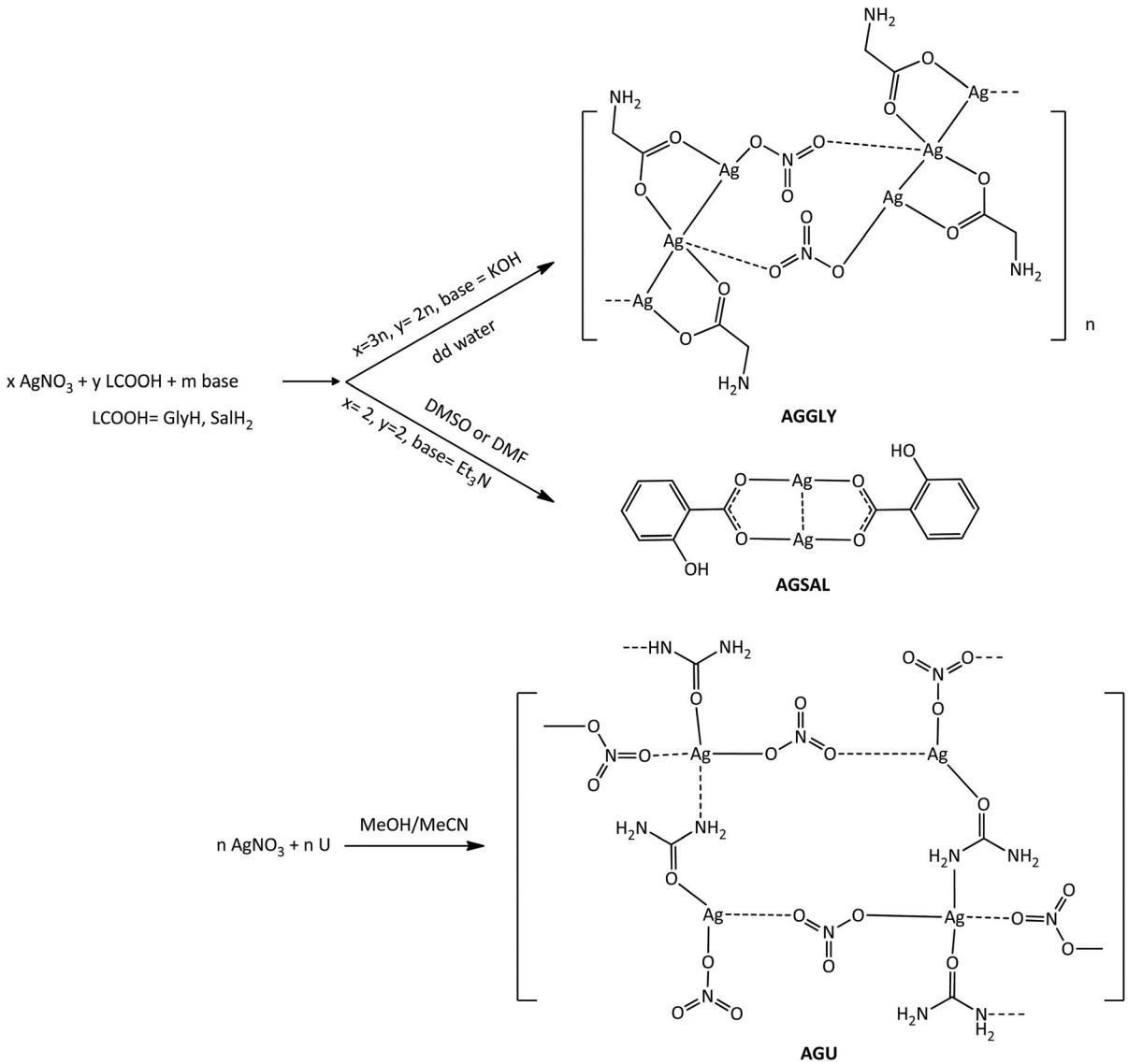

Scheme 1 Reaction route for the synthesis of **AGGLY**, **AGU** and **AGSAL**.

Ag Kα X-ray emission was used for the quantitative determination of Ag. The content of silver in **pHEMA@AGGLY-2**, **pHEMA@AGU-2** and **pHEMA@AGSAL-2** was determined to be 0.19 ± 0.05, 0.16 ± 0.04 and 0.23 ± 0.05% w/w, while the calculated one is 0.11 (**pHEMA@AGGLY-2**), 0.04 (**pHEMA@AGU-2**) and 0.08 (**pHEMA@AGSAL-2**) % respectively. The variations between the experimental and calculated values are due to its low quantity, which is close to the limits of the method.

X-ray powder diffraction analysis (XRPD)

Powders of dry **pHEMA@AGGLY-2**, **pHEMA@AGU-2** and **pHEMA@AGSAL-2** discs were used for XRPD spectra recording (Fig. S5–S7†). The absence of diffraction in the XRPD spectra of **pHEMA@AGGLY-2**, **pHEMA@AGU-2** and **pHEMA@AGSAL-2**, such as those observed in the XRPD diagrams of their corresponding ingredients **AGGLY**, **AGU** and **AGSAL** shows either the effective phase transition from the crystalline to amorphous phase during confinement into pHEMA or their low concentrations in the disc.

Solid state UV-vis spectra

The dispersion of **AGGLY**, **AGU** and **AGSAL** in pHEMA within **pHEMA@AGGLY-2**, **pHEMA@AGU-2** and **pHEMA@AGSAL-2** was verified by solid state UV-Vis spectroscopy (Fig. S8†). The characteristic bands in the solid state UV-Vis spectra of pHEMA (240 nm) and free ingredients **AGGLY** (280 nm), **AGU** and **AGSAL** (280, 295 and 295 nm respectively) undergo a hypsochromic shift in the cases of **pHEMA@AGGLY-2**, **pHEMA@AGU-2** and **pHEMA@AGSAL-2** (230, 210 and 240 nm respectively) suggesting the incorporation of the silver complexes in pHEMA.

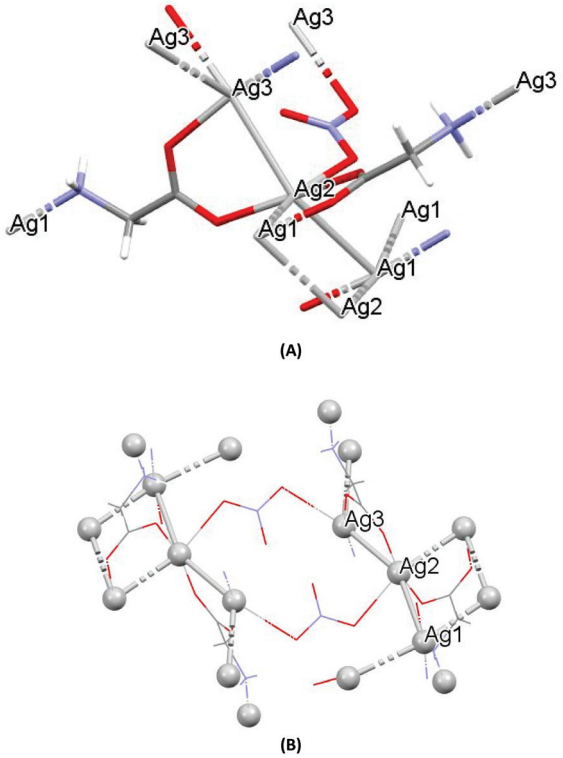

Fig. 1 (A) Molecular diagrams of **AGGLY**. (B) Covalent Ag–O and Ag–N intra-molecular interactions lead to supramolecular assembly.

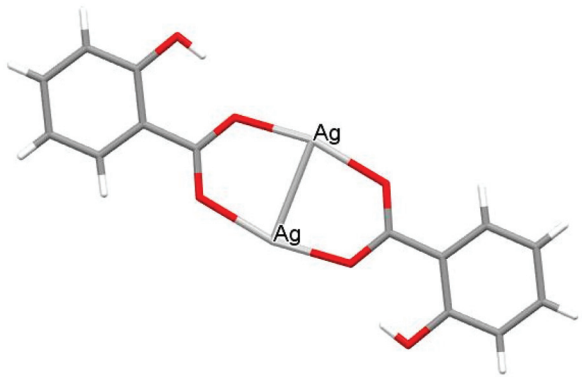

Fig. 2 Molecular diagram of **AGSAL**.

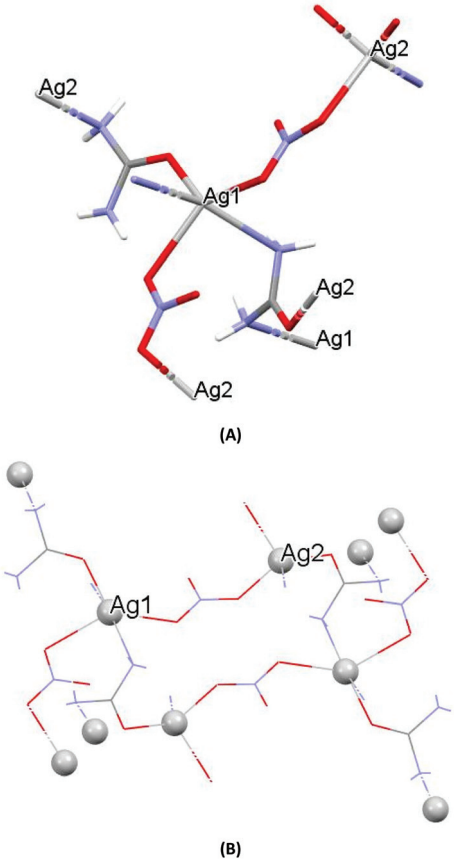

Fig. 3 (A) Molecular diagram of **AGU**. Selected bond lengths (Å) and angles [°]: Ag1–O1 = 2.492(7), Ag1–O2 = 2.845(6), Ag1–O4 = 2.425(5), Ag1–O8 = 2.340(5), Ag1–N4 = 2.636(8), Ag1–N3_d = 2.657(8), O1–Ag1–O2 = 47.44(16), O1–Ag1–O4 = 130.89(19), O1–Ag1–O8 = 97.40(19), O1–Ag1–N4 = 91.6(2), O1–Ag1–N3_d = 81.2(2). (B) Covalent Ag–O and Ag–N intra-molecular interactions lead to supramolecular assembly.

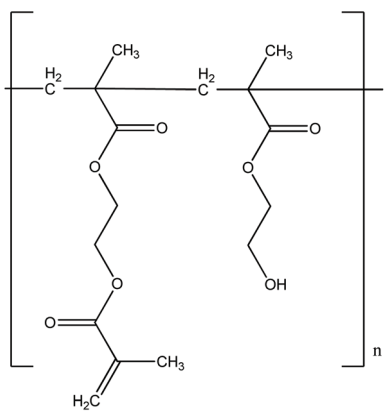

Poly(EDGMA-HEMA)
(pHEMA)

Scheme 2 pHEMA.

Thermo-gravimetric analysis of biomaterials pHEMA@AGGLY-2, pHEMA@AGU-2 and pHEMA@AGSAL-2

Differential scanning calorimetry (DSC). In order to clarify whether **AGGLY**, **AGU** and **AGSAL** and pHEMA interact in the solid state to give a composite material or a mixture, DSC studies were carried out on the powders of dry pHEMA and **pHEMA@AGGLY-2**, **pHEMA@AGU-2** and **pHEMA@AGSAL-2** discs. The DSC thermodiagrams are shown in Fig. 4. The endothermic transition which is observed at 415.39 °C in the DSC diagram of pHEMA is shifted to lower temperatures of 396.77 and 408.92 °C for **pHEMA@AGGLY-2** and **pHEMA@AGU-2** respectively implying an interaction between the material's components and therefore the formation of composite materials. In contrast no differences were observed

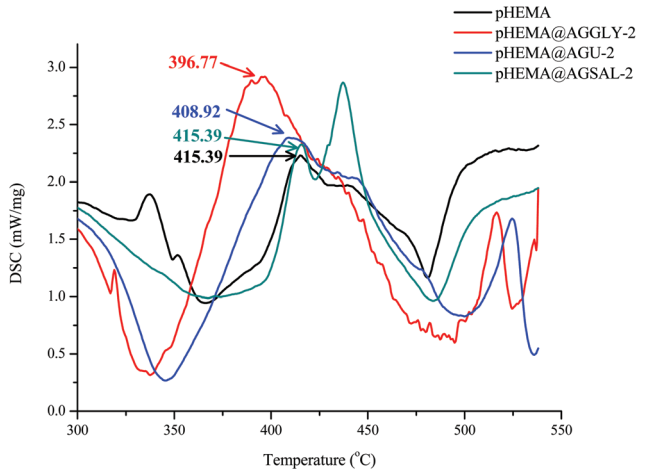

Fig. 4 DSC diagrams on the powders of dry pHEMA and **pHEMA@AGGLY-2**, **pHEMA@AGU-2** and **pHEMA@AGSAL-2** discs.

between the DSC diagrams of pHEMA and **pHEMA@AGSAL-2**, suggesting the formation of a mixture in this case.

Thermal decomposition. TG/DTA analysis was performed under air on the dry powders of **pHEMA@AGGLY-2**, **pHEMA@AGU-2** and **pHEMA@AGSAL-2**, upon increasing the temperature at a rate of 10 °C min^{-1} from ambient up to 500 °C (Fig. S9†). The two covalent polymer biomaterials **pHEMA@AGGLY-2** and **pHEMA@AGU-2** decompose within five endothermic steps at mid temperatures of 171.7, 297.2, 393.7, 438.1, and 544.9 °C (**pHEMA@AGGLY-2**) and 183.9, 294.0, 390.8, 438.5, and 516.1 °C (**pHEMA@AGU-2**) respectively, while dimeric **pHEMA@AGSAL-2** decomposes within four endothermic steps at mid temperatures of 183.9, 186.7, 282.2, 398.8, and 459.2 °C.

Antibacterial activity

Minimum inhibitory concentration (MIC). The antibacterial efficiency of the agents was evaluated by using their minimal inhibitory concentration (MIC) values against the Gram-negative species *P. aeruginosa* and Gram positive ones *S. epidermidis* and *S. aureus* upon their incubation for 20 h. These microbes are abundant in microbial keratitis. The MIC values of **AGSAL** were determined previously.[13] **AGSAL** and **AGGLY** exhibit higher antimicrobial activity than silver nitrate, a disinfectant-antiseptic formulation in clinical use, which increases up to 2.8-, 1.2- and 1.4-fold against *P. aeruginosa, S. epidermidis* and *S. aureus*, respectively (Table 1 and Fig. S10†). In contrast, **AGU** exhibits moderate activity, which is the half of that of $AgNO_3$ against all microbes tested *P. aeruginosa*, *S. epidermidis* and *S. aureus* respectively. GlyH, $SalH_2$ and U show no antibacterial activity at concentrations up to 200 μM (Fig. S11–S13†).[13] Microbes are classified as susceptible (MIC < 50 μM) or resistant (MIC > 100 μM) towards an antimicrobial agent by their MIC values. Therefore *P. aeruginosa, S. epidermidis* and *S. aureus* are susceptible to **AGGLY** and **AGSAL** but they are resistant towards **AGU**.

Minimum bactericidal concentration (MBC). The MBC value, which is the lowest concentration of antibacterial agents that kills 99.9% of the initial bacterial inoculums, was determined for **AGGLY** and **AGU**.[5,8,9,13–15,27] The MBC values of **AGSAL** were determined previously.[13] The MBC values of the agents are shown in Table 1 (Fig. S14†). The bactericidal activity of the tested agents is stronger than tat of silver nitrate, and in the cases of **AGGLY** and **AGSAL** it reaches 5.5- and 4.6-fold respectively towards *P. aeruginosa* (Table 1). The MBC/MIC value of an agent is used for its classification as bactericidal and bacteriostatic ones. Thus, a bactericidal agent that kills 99.9% of the microorganisms shows an MBC/MIC value of ≤2. In contrast, in the case of a bacteriostatic agent, which inhibits but not kills the organism, the MBC/MIC value is ≥4.[5,8,9,13–15,27] The MBC/MIC values for the tested microbes **AGGLY**, **AGU** and **AGSAL** lie in the range from 1.10 to 1.52 which classified them as bactericidal ones (Table 1).

Viability of microbes upon their incubation with biomaterials. Due to the antimicrobial activity of the conjugates of silver(I) ions with amino acids, metabolites or natural product ingredients (such as GlyH, U and $SalH_2$), **AGGLY**, **AGU** and **AGSAL** were dispersed in pHEMA aiming for the development of new non infected soft contact lens materials. The discs of pHEMA, **pHEMA@AGGLY-2**, **pHEMA@AGU-2**, **pHEMA@AGSAL-2**, were placed in tests tubes with the bacterial strains *P. aeruginosa*, *S. epidermidis* and *S. aureus* (Fig. 5). Discs of the corresponding **pHEMA@Gly-2**, **pHEMA@U-2** and **pHEMA@SalH$_2$-2**, were prepared similarly by the dispersion of **GlyH**, **U** and **SalH$_2$** in 2 mM and they were used for comparison (Fig. 5).

The calculated % bacterial viability of *P. aeruginosa, S. epidermidis and S. aureus* upon their incubation with the new biomaterials **pHEMA@AGGLY-2**, **pHEMA@AGU-2**, and **pHEMA@AGSAL-2** is extremely low in the range of 0.8–1.2%, 2.1–5.2% and 2.4–3.3% against *P. aeruginosa, S. epidermidis and S. aureus*, respectively (Table 1). The *P. aeruginosa* and *S. aureus* are eliminated by the discs of **pHEMA@AGU-2**, up to 99.2 and 97.6%, respectively, while the bacteria of *S. epidermidis* are eliminated by the disc of **pHEMA@AGSAL-2** up to 97.6%. No influence on the bacterial viability was observed upon their treatment with the discs of pure pHEMA or pHEMA@Gly-2, pHEMA@U-2 and pHEMA@$SalH_2$-2 (Fig. 5). However, bacterial colonies of *P. aeruginosa, S. epidermidis* and *S. aureus* are grown in agar plates when 4 μL of the supernatants of the solutions were used, which were initially treated with the discs of pHEMA and **pHEMA@AGGLY-2**, **pHEMA@AGU-2**, and **pHEMA@AGSAL-2** (Fig. 6). Therefore, the biomaterials prohibit microbial growth only when they are present in the microbe cultures (Fig. 8).

Inhibition zone (IZ). In order to confirm the bacterial elimination in the presence of the biomaterials the agar disk-diffusion method was employed against *P. aeruginosa*, *S. epidermidis* and *S. aureus*.[5,8,9,13–15,27] The diameters of the bacterial growth inhibition zones, when the tested strains are treated with the ingredients of the biomaterials **AGGLY**, **AGU** and **AGSAL** upon their incubation for 20 h, are summarized in Table 1 (Fig. 7).

Table 1 MICs, MBCs, IZs, BEC, and bacterial viability of **AGGLY**, **AGU**, **AGSAL**, **pHEMA@AGGLY-2**, **pHEMA@AGU-2** and **pHEMA@AGSAL-2** against *P. aeruginosa*, *S. epidermidis* and *S. aureus*. IC_{50} (μM) values of **AGGLY**, **AGU**, and **AGSAL** towards HCECs

	P. aeuroginosa	*S. epidermidis*	*S. aureus*	Ref.
	MIC (μM)			
AGGLY	21.4 ± 4.6	49.6 ± 6.6	51.3 ± 5.1	[a]
AGU	94.6 ± 3.9	90.3 ± 10.7	92.0 ± 10.4	[a]
AGSAL	28.0	50.0	42.0	13
$AgNO_3$	60.0	122.0	95.0	13 and 14
	MBC (μM)			
AGGLY	28.0 ± 4.5	55.0 ± 9.0	75 ± 0	[a]
AGU	120 ± 14	132 ± 16	140 ± 23	[a]
AGSAL	33	90	50	13
$AgNO_3$	153.3 ± 13.1	140	135.0 ± 6.7	13 and 14
	MBC/MIC			
AGGLY	1.31	1.11	1.46	[a]
AGU	1.27	1.46	1.52	[a]
AGSAL	1.18	1.80	1.19	13
$AgNO_3$	2.56	1.15	1.42	13 and 14
	Bacterial viability (%)			
pHEMA@AGGLY-2	1.2	5.2	3.3	[a]
pHEMA@AGU-2	0.8	4.9	2.4	[a]
pHEMA@AGSAL-2	1.1	2.1	3.1	[a]
	IZ (mm)			
AGGLY (1 mM)	11.7 ± 1.8	13.0 ± 1.9	12.5 ± 0.9	[a]
AGGLY (2 mM)	13.9 ± 1.6	16.4 ± 1.6	15.3 ± 1.7	[a]
AGU (1 mM)	12.5 ± 0.9	12.3 ± 1.7	14.0 ± 1.7	[a]
AGU (2 mM)	14.3 ± 1.5	14.5 ± 1.7	16.1 ± 1.3	[a]
AGSAL (1 mM)	13.0	13.0	12.0	13
AGSAL (2 mM)	13.4 ± 1.5	14.7 ± 1.3	13.8 ± 1.4	[a]
pHEMA@AGGLY-2	12.4 ± 1.0	12.2 ± 1.1	12.5 ± 1.0	[a]
pHEMA@AGU-2	14.5 ± 1.0	14.5 ± 1.0	13.3 ± 1.8	[a]
pHEMA@AGSAL-2	14 ± 1.9	15.2 ± 0.3	14.3 ± 2.4	[a]
	BEC (μM)			
AGGLY	150 ± 22	—	294 ± 4	
AGU	694 ± 139	—	687 ± 38	[a]
AGSAL	875		648	13
HCIP·HCl	670		952	27
HCIP	2140		2463	27
	IC_{50} (μM) towards HCECs			
AGGLY		2.87 ± 0.13		[a]
AGU		8.69 ± 0.65		[a]
AGSAL		10.22 ± 0.33		[a]

[a] In this work; HCIP·HCl = ciprofloxacin hydrochloride and HCIP = ciprofloxacin.

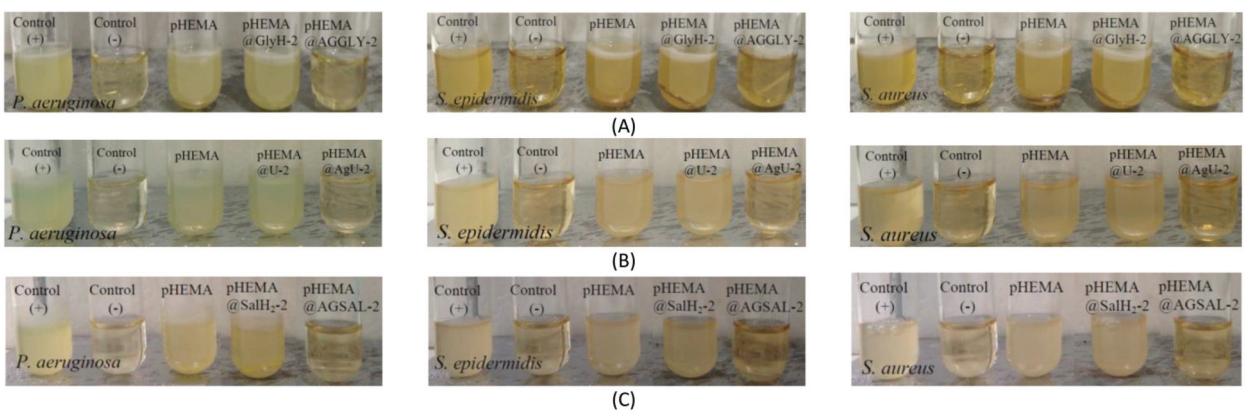

Fig. 5 Bacterial (*P. aeruginosa*, *S. epidermidis* and *S. aureus*) viability when they are incubated over pHEMA; A: **pHEMA@GlyH-2** and **pHEMA@AGGLY-2**; B: **pHEMA@U-2** and **pHEMA@AGU-2** and C: **pHEMA@$SalH_2$-2** and **pHEMA@AGSAL-2** under continuous stirring.

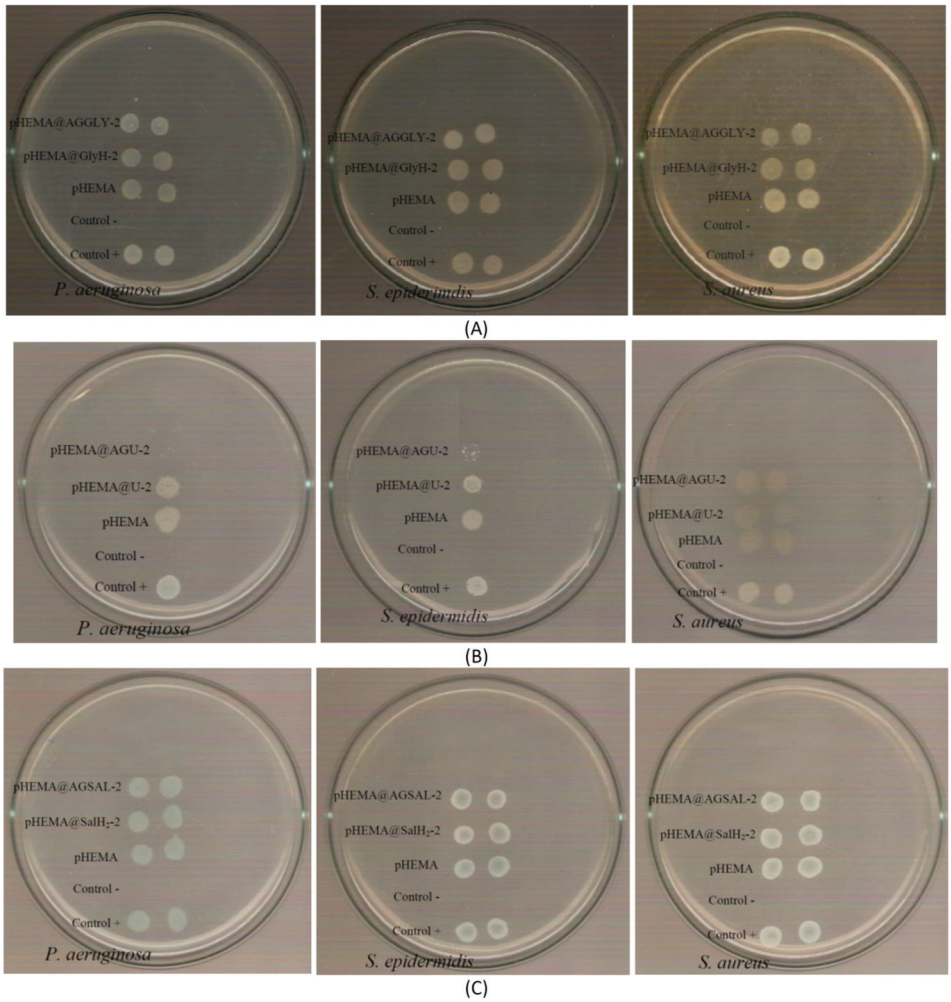

Fig. 6 Bacterial colonies of *P. aeruginosa, S. epidermidis* and *S. aureus* grown in agar plates when 4 μL of the supernatants of the solutions were used, which were initially treated with discs of pHEMA and **pHEMA@AGGLY-2** (A), **pHEMA@AGU-2** (B) and **pHEMA@AGSAL-2** (C).

The bacteria tested show higher sensitivity to the concentration of 2 mM than 1 mM for the biomaterial ingredients **AGGLY**, **AGU** and **AGSAL**. Therefore, these strains exhibit dose dependent response on the agents. No inhibition zones were developed when the microbes were incubated with glycine, urea and salicylic acid at 1 or 2 mM. The Gram positive bacteria possess higher sensitivity to the agents than the corresponding negative ones. Particularly, **AGGLY** and **AGSAL** develop greater IZ towards *S. epidermidis*, (IZ 16.4 ± 1.6 and 14.7 ± 1.3 mm, respectively) while **AGU** exhibits the highest activity against *S. aureus* with an IZ value of 16.1 ± 1.3 mm. The microbial strains are classified into three categories according to the size of IZ, caused by an antimicrobial agent in their agar dilution culture: (i) strains, where the agent causes IZ ≥ 17 mm, are susceptible, (ii) those where an agent creates IZ between 13 and 16 mm (13 ≤ IZ ≤ 16 mm) are intermediate, while (iii) those where the agent causes IZ ≤ 12 mm are considered as resistant ones.[5,8,9,13–15,27] Therefore, the response of *P. aeruginosa*, *S. epidermidis* and *S. aureus* can be considered as an intermediate against **AGGLY**, **AGU** and **AGSAL** at both concentrations used (1 or 2 mM).

The inhibition zones which were developed in agar plates of *P. aeruginosa*, *E. coli*, *S. epidermidis* and *S. aureus* microbes around the **pHEMA@AGGLY-2**, **pHEMA@AGU-2** and **pHEMA@AGSAL-2** discs suggest mild antimicrobial activity (Table 1 and Fig. 8). Moreover, no inhibition zones were developed when pHEMA or **pHEMA@Gly-2**, **pHEMA@U-2** and **pHEMA@SalH$_2$-2** were used against the bacterial strains (Table 1 and Fig. 8).

The IZs of **pHEMA@AGU-2** and **pHEMA@AGSAL-2** hydrogels are similar to those of the soaked paper discs with the ingredient solutions (2 mM). In the case of the **pHEMA@AGGLY-2** discs, however, the IZs developed against *P. aeruginosa*, *E. coli*, *S. epidermidis* and *S. aureus* (12.4 ± 1.0, 12.2 ± 1.1 and 12.5 ± 1.0 mm) are shorter than the soaked paper discs with **AGGLY** (2 mM) (13.9 ± 1.6, 16.4 ± 1.6 and 15.3 ± 1.7 mm), respectively. This suggests the negligible release of the disc ingredient.

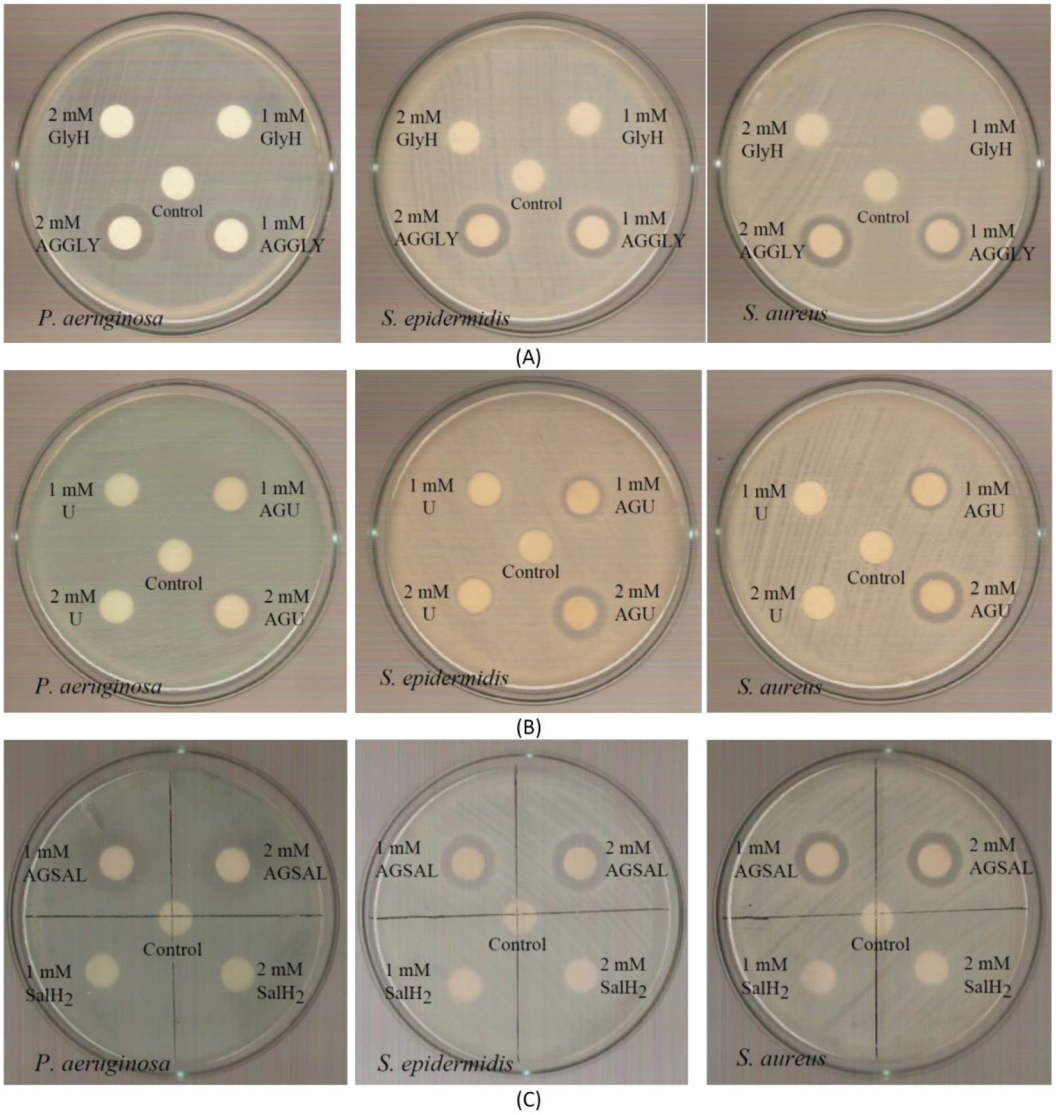

Fig. 7 IZs which are developed in agar plates of *P. aeruginosa*, *S. epidermidis* and *S. aureus* by the **AGGLY**, GlyH (A), **AGU**, urea (B) and **AGSAL**, $SalH_2$ (C) at 1 and 2 mM.

Effect of biomaterials on biofilm formation. Since the biofilm formation on contact lens surfaces hardens the treatment of keratitis,[28] the effect of biomaterials on biofilm formation was evaluated towards *P. aeruginosa* and *S. aureus.* It is pointed out that these are the positive strains for biofilm formation.[9] The biofilm elimination concentration (BEC) of the antimicrobial agents was determined as the concentration required to achieve at least a 99.9% reduction in the viability of biofilm bacteria.[9] The biomaterials **AGGLY** and **AGU** can inhibit biofilm formation with BECs of 150 and 694 μM, respectively against *P. aeruginosa*, while their BEC values against *S. aureus* are 294 and 687 μM, respectively (Table 1 and Fig. S15†). The BEC values of **AGSAL** were determined previously[13] being 875 μM for *P. aeruginosa* and 648 μM for *S. aureus* (Table 1). Among the tested biomaterials, **AGGLY** is more effective than ciprofloxacin hydrochloride (HCIP-HCL) (up to 4.5 and 3.2-fold against *P. aeruginosa* and *S. aureus*) and it is more effective than ciprofloxacin (HCIP) (up to 14.3 and 8.4-fold against *P. aeruginosa* and *S. aureus*).

The biofilm formation on the surface of contact lenses increases the survival of the bacteria and their replication on the lens surface.[28] *In vitro* studies have demonstrated that the bacteria can adhere to all types of contact lenses.[28] The percent of removal of the preformed biofilm was assessed using the crystal violet assay.[5] The discs of **pHEMA@AGGLY-2**, **pHEMA@AGU-2** and **pHEMA@AGSAL-2** eliminate the biofilm of *P. aeruginosa* by 40.3, 27.5 and 39.7%, respectively while they eliminate the biofilm of *S. aureus* by 42.0, 24.1 and 23.2%, respectively; no inhibitory activity is observed against the biofilm of *S. aureus* (Fig. 9).

***In vitro* toxicity against normal human corneal epithelial cells (HCECs).** The toxic effect of the biomaterial discs was evaluated towards normal human corneal epithelial cells

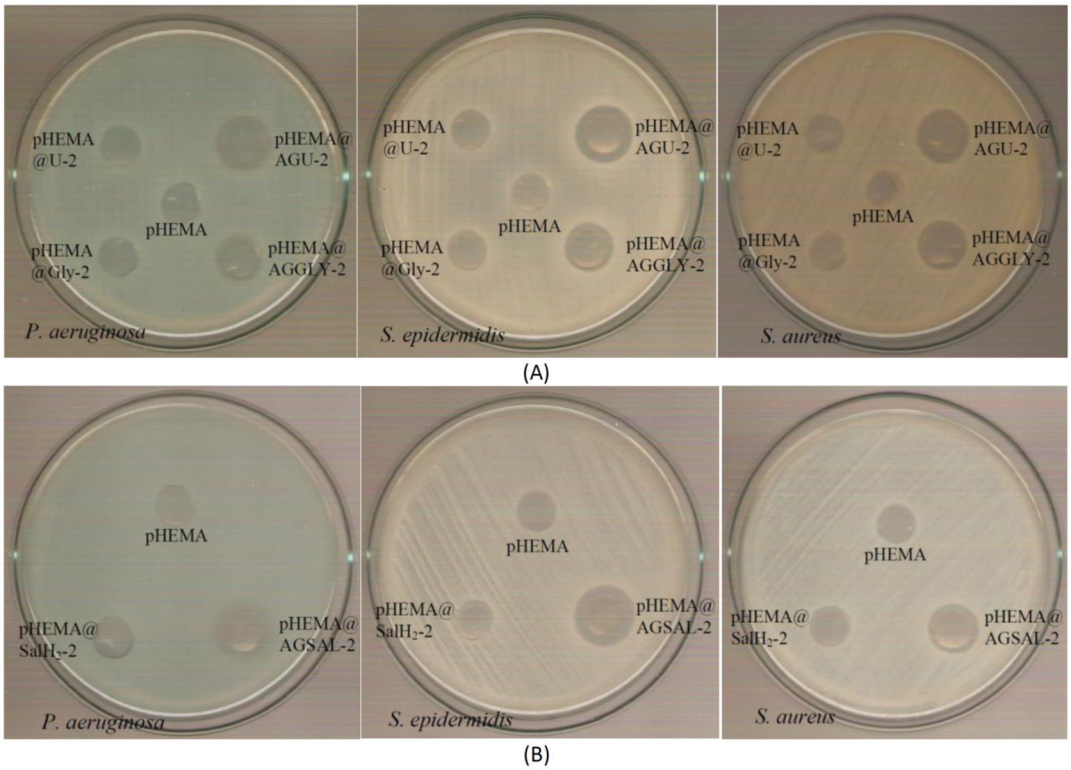

Fig. 8 IZs which are developed around pHEMA (A and B), **pHEMA@AGGLY-2**, **pHEMA@AGU-2**, **pHEMA@GlyH-2**, **pHEMA@U-2** (A) and **pHEMA@AGSAL-2** and **pHEMA@SalH$_2$-2** (B) discs in agar plates of *P. aeruginosa*, *S. epidermidis* and *S. aureus*.

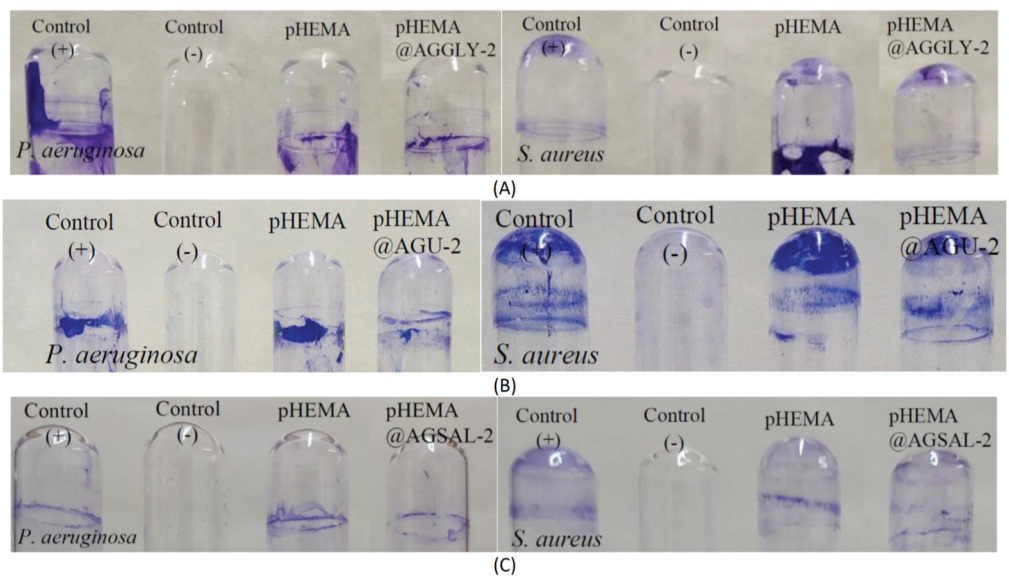

Fig. 9 Biofilms of *P. aeruginosa* and *S. aureus elimination* caused by **pHEMA@AGGLY-2** (A), **pHEMA@AGU-2** (B) and **pHEMA@AGSAL-2** (C) discs.

(HCEC) after their incubation for a period of 48 h. The IC_{50} values of **AGGLY**, **AGU** and **AGSAL** are in the range of 2.87–10.22 μM (Table 1). Moreover, the cell viability of HCEC upon their incubation with the discs of **pHEMA@AGGLY-2**, **pHEMA@AGU-2** and **pHEMA@AGSAL-2** was estimated for 24 and 48 h. The corresponding cell viability of the discs at 24 h was 84.2 ± 1.9, 98.8 ± 2.7 and 95.4 ± 3.0% for **pHEMA@AGGLY-2**, **pHEMA@AGU-2** and **pHEMA@AGSAL-2**, respectively. Therefore a negligible cytotoxic effect of the discs towards normal cells is observed. However, the cytotoxicity

slightly increases (57.6 ± 2.2, 100 ± 0.0 and 74.0 ± 4.3% respectively) when HCECs were treated with the discs for 48 h.

***In vitro* genotoxicity of biomaterials against normal human corneal epithelial cells (HCECs).** The genotoxicity test identifies the mutagenicity level of an agent.[29] A biomarker for the mutagenic, genotoxic, or teratogenic influence of an agent is the presence of micronucleus (MN) which is formed from the chromosome breakage and/or whole chromosome loss.[30] Therefore the *in vitro* genotoxicity was evaluated by checking the micronucleus (MN) frequency, upon treatment of HCECs in the presence of biomaterials for a period of 48 h.[31] The MN frequency in the untreated and treated HCECs with pHEMA, is 1.28 ± 0.06 and 1.76 ± 0.40% respectively. The corresponding frequency was slightly increased upon treatment of the cells with **pHEMA@AGGLY-2**, **pHEMA@AGU-2** and **pHEMA@AGSAL-2** (2.41 ± 0.36, 2.26 ± 0.44 and 2.12 ± 0.25%,

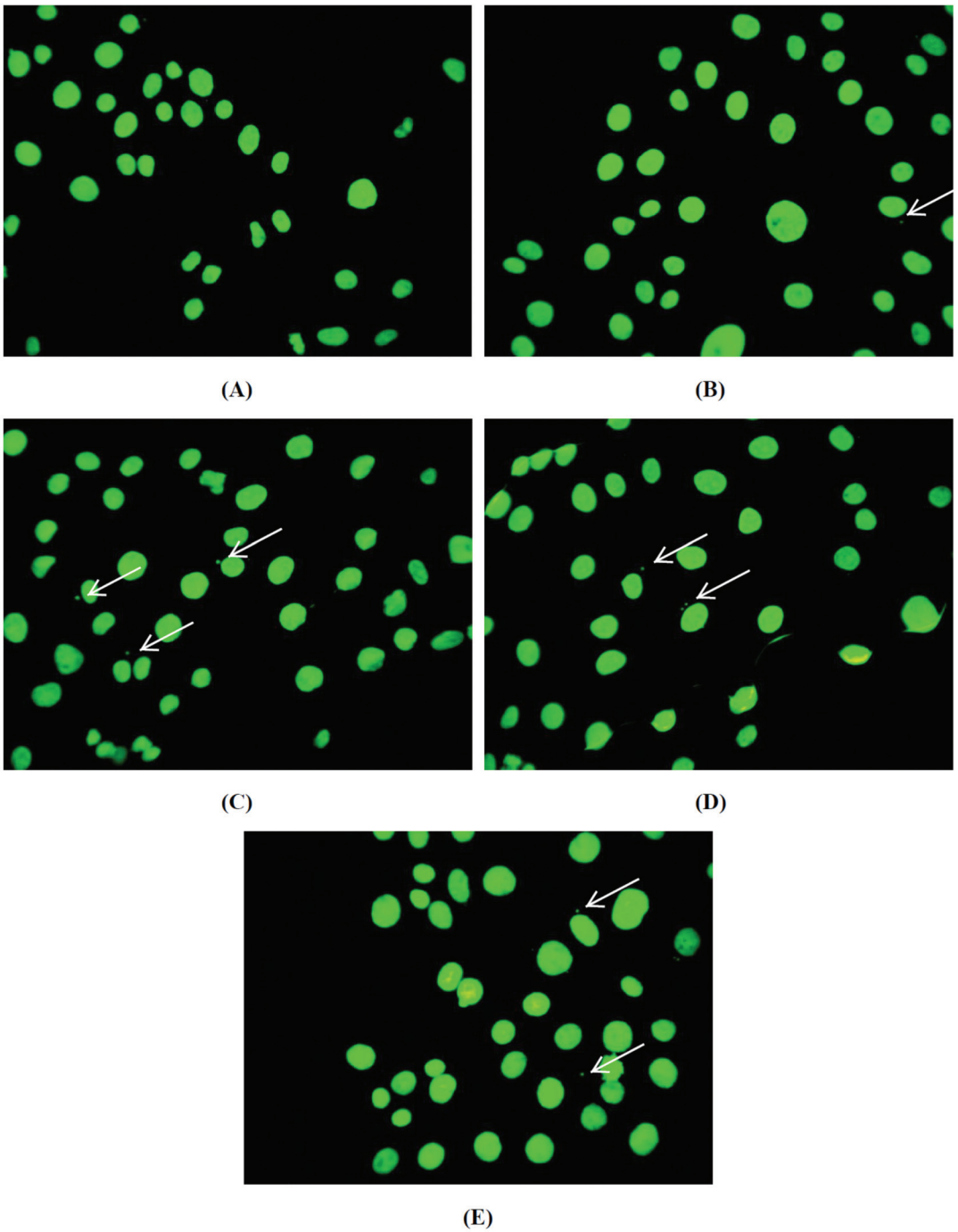

Fig. 10 Micronucleus formed in untreated HCECs (A) and upon their treatment with pHEMA (B), **pHEMA@AGGLY-2** (C), **pHEMA@AGU-2** (D) and **pHEMA@AGSAL-2** (E), for a period of 48 h; the arrow indicates the micronucleus in HCECs.

Table 2 The mitotic index% (MI) and the chromosomal aberrations% (CA) observed when *Allium cepa* was incubated with pHEMA, **pHEMA@AGGLY-2**, **pHEMA@AGU-2** and **pHEMA@AGSAL-2** for 48 h

	MI	CA
Untreated cells	7.3 ± 1.0	0.9 ± 0.3
pHEMA	6.8 ± 1.7	0.9 ± 0.4
pHEMA@AGGLY-2	7.2 ± 1.3	1.1 ± 0.5
pHEMA@AGU-2	6.5 ± 1.0	1.0 ± 0.1
pHEMA@AGSAL-2	6.4 ± 0.5	0.4 ± 0.1

respectively) (Fig. 10). Therefore, a low *in vitro* genotoxic effect of the studied biomaterials here is concluded.

***In vivo* toxicity of biomaterials on brine shrimp *Artemia salina*.** A simple and suitable model for the acute toxicity screening of materials, nanoparticles and metal complexes is the nauplii of the brine shrimp *Artemia salina.*[5,8,15,32–36] *Artemia salina* is a zooplanktonic crustacean.[32]

After the incubation of brine shrimp larvae with the biomaterials, pHEMA, **pHEMA@AGGLY-2**, **pHEMA@AGU-2** and

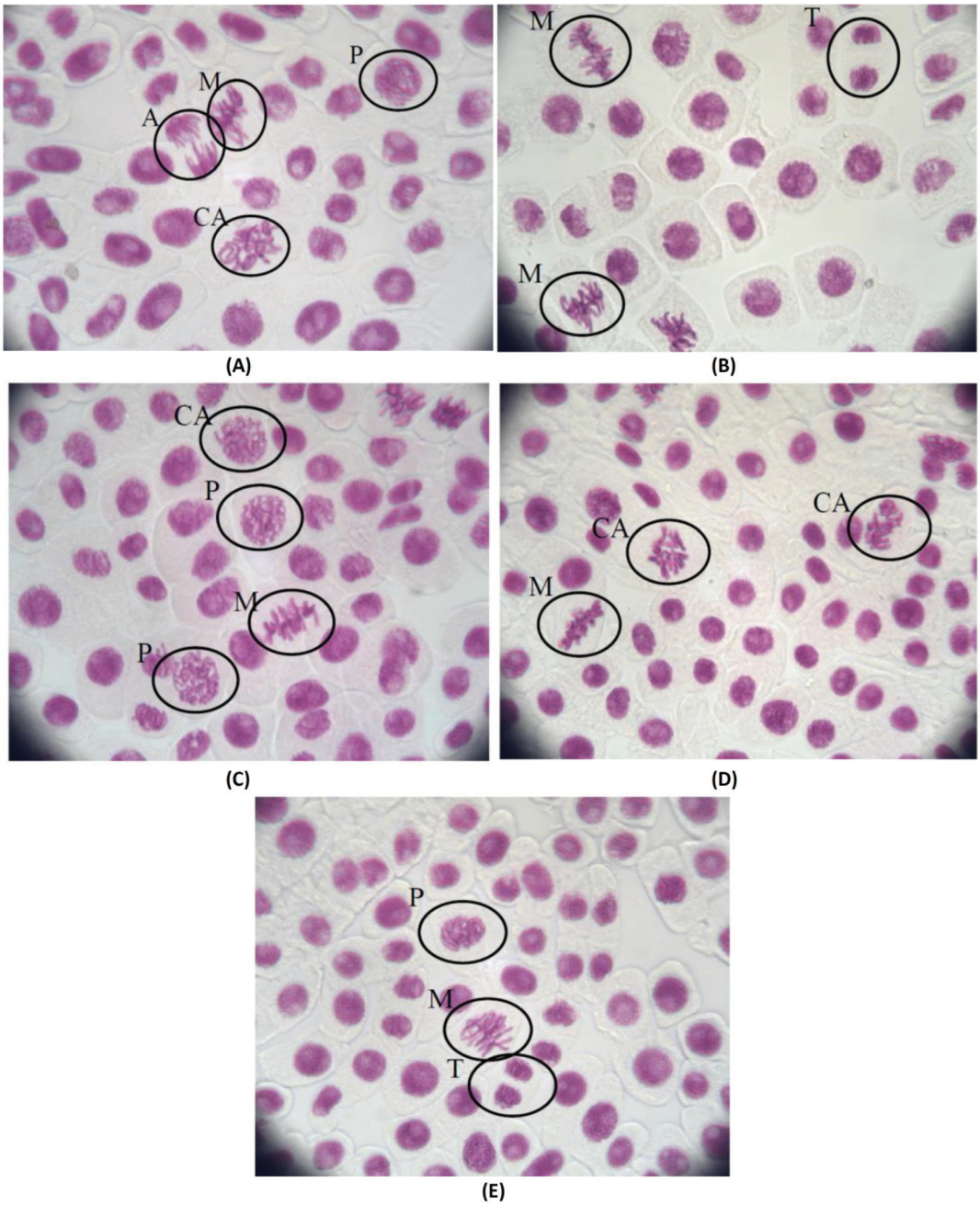

Fig. 11 *Allium cepa* meristematic cells exposed to biomaterials. Untreated *Allium cepa* meristematic cells (A) (P = prophase, A = anaphase, M = metaphase, T = telophase and CA = chromosomal aberration). *Allium cepa* meristematic cells exposed with pHEMA (B), **pHEMA@AGGLY-2** (C), **pHEMA@AGU-2** (D), and **pHEMA@AGSAL-2** (E).

pHEMA@AGSAL-2, for a period of 24 h, no mortality level was found. Thus a non-toxic behaviour of the biomaterial discs is suggested.

***In vivo* genotoxicity study of the biomaterials on *Allium cepa*.** The use of plants, such as *Allium cepa*, as a bioindicator has been standardized by the United Nations Environment Program and the Environmental Protection Agency's (EPA) international programs.[37] EPA and the World Health Organization acknowledge the data from these bioassays as effective and reliable ones for the evaluation of potential genotoxicity *in vivo*.[37] *Allium cepa* displays a high correlation with mammal test systems because of their similarity in chromosomal morphology.[31,38] The assay is useful to identify the damaging effect or to evaluate the influence of a material on *in vivo* systems.[9,12–14,22,27,31] In order to evaluate the toxicity, the mitotic index (%) and DNA damage such as chromosomal aberrations (%) and nuclear abnormalities (%) are determined when *Allium cepa* bulbs are treated with pHEMA, **pHEMA@AGGLY-2**, **pHEMA@AGU-2** and **pHEMA@AGSAL-2** for 48 h (Table 2).

The mitotic index and the chromosomal aberrations of the cell division of *Allium cepa* are not affected when they are treated with **pHEMA@AGGLY-2**, **pHEMA@AGU-2** and **pHEMA@AGSAL-2** for 48 h, indicating that the biomaterials are not mutagenic or genotoxic (Fig. 11). The mitotic indexes of the treated *Allium cepa* meristematic root cells with **pHEMA@AGGLY-2**, **pHEMA@AGU-2** and **pHEMA@AGSAL-2** are 7.2 ± 1.3, 6.5 ± 1.0 and 6.4 ± 0.5%, respectively. These values are in accordance with those of the untreated group or the group treated with pHEMA (7.3 ± 1.0 and 6.8 ± 1.7%, respectively). Therefore no *in vivo* genotoxic effect can be concluded for the new biomaterials.

Conclusion

Since the contact lens wear can be implicated with the occurrence of microbial keratitis (MK), novel active biomaterials **pHEMA@AGGLY-2**, **pHEMA@AGU-2**, and **pHEMA@AGSAL-2** were synthesised by the dispersion in pHEMA of the known water soluble silver(I) covalent polymers **AGGLY**, **AGU** and **AGSAL** of the natural products GlyH, U and $SalH_2$.

The silver(I) covalent polymers were tested for the antibacterial efficiency against microbes which colonise in contact lenses. **AGGLY** and **AGSAL** exhibit higher antimicrobial activity than silver nitrate, which increases up to 2.8-, 1.2- and 1.4-fold against *P. aeruginosa*, *S. epidermidis* and *S. aureus*, respectively (Table 1). In contrast, **AGU** exhibits moderate activity against the tested microbes. The MBC/MIC values of **AGGLY**, **AGU** and **AGSAL** classified them as bactericidal ones (Table 1). **AGGLY**, **AGU** and **AGSAL** were dispersed in pHEMA aiming for the development of new non infected soft contact lens materials. The biomaterials can eliminate up to 94.8–99.2% of the bacteria after their incubation with the hydrogels. This activity is superior to those exhibited by pHEMA@(SLS@[$Zn_3(CitH)_2$]) ($CitH_4$ = citric acid; SLS = sodium lauryl sulphate) which were found to lie between 6.5 and 29.0% respectively, pHEMA@ORLE_2 (ORLE = oregano leaf extract) and pHEMA@AgNPs(ORLE)_2 (AgNPs(ORLE) = silver nanoparticles of oregano leaf extract) which were evaluated at 59.6–88.3% against *P. aeruginosa*, *S. epidermidis* and *S. aureus* which lie between 6.5 and 29.0% respectively.[8,10] However, the activity of **pHEMA@AGGLY-2**, **pHEMA@AGU-2**, and **pHEMA@AGSAL-2** is comparable to that of the corresponding pHEMA@AGMNA-1 (**AGMNA** = $\{[Ag_6(\mu_3\text{-HMNA})_4(\mu_3\text{-MNA})_2]^{2-}\cdot[(Et_3NH)^+]_2\cdot(DMSO)_2\cdot(H_2O)\}$) which was found to eliminate bacterial strains such as *P. aeruginosa*, *S. epidermidis* and *S. aureus* by 92.3–99.6% respectively.[5] Moreover, the biomaterials **pHEMA@AGGLY-2**, **pHEMA@AGU-2**, and **pHEMA@AGSAL-2** exhibit a low *in vitro* genotoxic effect against HCECs and negligible *in vivo* toxicity against *Artemia salina* and *Allium cepa* making them important candidates for the development of innovative non toxic biomaterials for sterilised contact lens preparation with high resistance against microbes which are involved in microbial keratitis.

Experimental

Materials and instruments

All solvents used were of reagent grade and were used with no further purification. Glycine, urea and salicylic acid were purchased from Sigma-Aldrich. Melting points were measured in open tubes with Stuart Scientific apparatus and are uncorrected. Mid infrared spectra (4000–400 cm^{-1}) were obtained on a Cary 670 FTIR spectrometer (Agilent Technologies). 2-Hydroxyethyl-methacrylate (pHEMA), ethylene-glycole-dimethacrylate (EGDMA, Merck), diphenyl(2,4,6-trimethylbenzoyl)phosphine oxide (TPO 97%, Sigma Aldrich) as well as sodium chloride (NaCl, Merck) and hydrochloric acid (HCl 37%, Merck) were used. X-ray fluorescence XRF measurements were carried out using an Am-241 radioisotopic source (exciting radiation 59.5 keV). For the detection of X-ray fluorescence, a Si (Li) detector was used. The measuring time was chosen to collect ~2000 data on the weaker Kα peak. The tryptone tryptophan medium, beef extract powder, bacteriological peptone, and soy peptone were purchased from Biolife. Agar and yeast extract were purchased from Fluka Analytical. Sodium chloride, D(+)-glucose, and di-potassium hydrogen phosphate trihydrate were purchased from Merck. Dulbecco's modified Eagle's medium, (DMEM), fetal bovine serum, glutamine and trypsin were purchased from Gibco, Glasgow, UK. Phosphate buffer saline (PBS) was purchased from Sigma-Aldrich. Dimethyl sulfoxide was purchased from Riedel-de Haën. For the toxicity experiments, Brine Shrimp Eggs (*Artemia salina*) were purchased from Ocean Nutrition.

Synthesis and crystallization of AGGLY, AGU and AGSAL

AGGLY and **AGSAL** were synthesized as described in a previous work.[13,22,23] For the synthesis of **AGU**, a solution of 0.5 mmol $AgNO_3$ (0.085 g) and 1 mmol urea (0.060 g) were stirred in

10 mL of methanol and 10 mL of acetonitrile. Crystals of pure **AGU** were grown from the slow evaporation of the solution.

AGGLY: Colorless crystal, melting point: 147–149 °C; Elemental analysis found: C: 9.30; H: 1.42, N: 7.70% calculated for $C_4H_8Ag_3N_3O_7$: C: 9.00; H: 1.51, N: 7.87%. IR (cm^{-1}): 3104w, 2426w, 2360w, 1764m, 1594s, 1496s, 1384vs, 1127m, 1043m, 930m, 891m, 826s, 667m, 506s; ^{1}H-NMR (ppm) in D_2O: 3.332 (s, C[H]; UV-vis (dd H_2O): λ = 194 nm ($\log \varepsilon$ = 4.86).

AGU: Colorless crystal, melting point: 90–100 °C; Elemental analysis found: C: 5.08; H: 1.90, N: 18.70%; calculated for $CH_4AgN_3O_4$: C: 5.22; H: 1.75, N: 18.28%; IR (cm^{-1}): 3437 (m), 2353 (m), 2170 (m), 1381 (vs), 1151 (m), 839 (m), 825 (m), 557 (w).

AGSAL: White-gray crystal, melting point: >280 °C; Elemental analysis found: C = 34.34, H = 2.11%; calc: C = 34.32, H = 2.06%; IR (cm^{-1}): 1588 (w), 1556 (s), 1455 (s), 1383 (m), 1334 (m), 1301 (m), 1257 (m), 1213 (w), 1141 (m), 1020 (w), 879 (w), 860 (s), 809 (s), 779 (s), 745 (w), 708 (vs), 667 (s), 546 (s), 475 (w), 423 (w), 407 (s), 394 (s), 377 (s); ^{1}H NMR (ppm) in D_2O: 7.77–7.75 (d, H[^{d}C], 7.41–7.37 (t, H [^{f}OH]), 6.92–6.87 (m, H[^{e,g}C]; UV–Vis (H_2O): λ = 202 nm ($\log \varepsilon$ = 2.5), λ = 228 nm ($\log \varepsilon$ = 1.82), λ = 295 nm ($\log \varepsilon$ = 1.38).

X-ray crystal structure determination

A crystal of **AGU**, (0.07 × 0.32 × 0.40 mm) was taken from the mother liquor and immediately cooled to −93 °C. Diffraction measurements for **AGU** were performed on a Rigaku R-AXIS SPIDER Image Plate diffractometer using graphite monochromated Mo Kα radiation.[39] Data collection (ω-scans) and processing (cell refinement, data reduction and empirical absorption correction) were performed using the CrystalClear program package. Important crystallographic data are listed in Table S3.† The structures were solved by direct methods using SHELXS v.2013/1 and refined by full-matrix least-squares techniques on F^2 with SHELXL ver. 2014/6.[40,41] Further experimental crystallographic details for **AGU**: $2\theta_{max}$ = 54.0°; reflections collected/unique/used, 14 437/2294 [R_{int} = 0.0321]/2294; 195 parameters refined; $(\Delta/\sigma)_{max}$ = 0.003; $(\Delta\rho)_{max}/(\Delta\rho)_{min}$ = 0.913/−0.704 e Å^{-3}; R_1/wR_2 (for all data), 0.0231/0.0475. All hydrogen atoms were located from difference Fourier maps and were refined freely. All non-hydrogen atoms were refined anisotropically. Plots of the structures were drawn using the Diamond 3 program package.[42]

Crystallographic data (excluding structure factors) for **AGU** reported in this paper have been deposited with the Cambridge Crystallographic Data Centre as supplementary publication no. CCDC 2089744.†

Synthesis of pHEMA@AGGLY-2, pHEMA@AGU-2 and pHEMA@AGSAL-2

Hydrogels of pHEMA incorporated with **AGGLY**, **AGU** and **AGSAL** were obtained as follows: 2.7 mL of HEMA was mixed with 2 mL of double distilled water (ddw), which contains **AGGLY**, **AGU** and **AGSAL** (2 mM) and 10 μL of EGDMA. The solution was then degassed by bubbling with nitrogen for 15 minutes. The TPO initiator (6 mg) was added to the solution and mixed for 5 min at 800 rpm. The solution was poured into the mold and was then placed under a UV mercury lamp (λ_{max} = 280 nm), 15 watt, where photopolymerization occurred, for 40 minutes. Unreacted monomers were removed, by immersing the gel in boiling water for 15 min. Discs with 10 mm diameter were cut, and they were washed by immersion in water, NaCl 0.9%, HCl 0.1 M, and again in water. The discs were then dried at 40 °C until no weight change would occur.

X-ray powder diffraction (XRPD)

The study of the samples by using X-ray powder diffraction was accomplished by using a diffraction-meter D8 Advance Bruker, Department of Physics, University of Ioannina. Radiation CuKα (40 kV, 40 mA, λKα) and the monochromator system of diffracted beam were used. The X-ray powder diffraction patterns were measured in the area of 2θ angles between 2° and 80° at a rotation step of 0.02° and time of 2 s per step. All samples measured with the above diffraction-meter were in the fine-grained powdered form.

Thermogravimetric differential thermal analysis (TG-DTA) and differential scanning calorimetry (DTG/DSC)

The measurements were performed on a DTG/TG NETZSCH STA 449C. For the measurements, 9.8, 9.2 and 14.6 mg of pHEMA@AGGLY-2, pHEMA@AGU-2 and pHEMA@AGSAL-2, respectively were placed inside a platinum capsule with alumina as the reference sample. The temperature increase rate was 10 °C min^{-1} in the range of 25–500 °C and the measurements were performed in an air atmosphere. The samples measured were in the fine-grained powdered form.

Biological tests

Bacterial strains. The bacterial strains of *P. aeruginosa*, *S. aureus* (ATCC® 25923™), and *S. epidermidis* (ATCC® 14990™), were adopted in the experiments. The bacterial strain *P. aeruginosa* was kindly offered from the Laboratory of Biochemistry, University of Ioannina-Greece. The biological experiments were performed in triplicate.

Effects on the growth of microbial strains. The procedure was performed as previously reported.[5,8,9,13–15,27] Briefly, bacterial strains plated onto trypticase soy agar medium (*P. aeruginosa* and *S. aureus*) or Luria–Bertani agar (LB agar) medium (*P. aeruginosa*) were incubated at 37 °C for 18–24 h. Three to five isolated colonies of the same morphological appearance were selected from a fresh agar plate using a sterile loop and transferred into a tube containing 2 mL of sterile saline solution. The optical density at 620 nm is adjusted to 0.1 which corresponds to 10^8 cfu mL^{-1}.[5,8,9,13–15,27] For the evaluation of MIC the inoculum size for broth dilution is 5×10^5 cfu mL^{-1}. The culture solution was treated with **AGGLY**, glycine, **AGU** and urea (8–200 μM). For the evaluation of MBC, the bacteria were initially cultivated in the presence of **AGGLY** and **AGU** in broth culture (Luria–Bertani agar (LB agar) medium) for 20 h. The MBC values were determined in duplicate, by subculturing 4 μL of the broth on an agar plate.[5,8,9,13–15,27]

In order to evaluate the viability of the microbes on the pHEMA, **pHEMA@AGGLY-2**, **pHEMA@AGU-2** and **pHEMA@AGSAL-2** discs, the materials were placed in the test tubes which contain 5×10^5 cfu mL^{-1} of the *P. aeruginosa*, *S. epidermidis* and *S. aureus* microbes.[5,8,9,13–15,27] The optical densities of the supernatant solutions were then measured to give the % viability of the microbes after incubation for 18–24 h.[5,8,9,13–15,27]

For the evaluation of IZ, **AGGLY**, glycine, **AGU**, urea at 1 mM and 2 mM, and the disks of pHEMA, **pHEMA@AGGLY-2**, **pHEMA@AGU-2** and **pHEMA@AGSAL-2** were placed on the agar surface and the Petri plates were incubated for 20 h.[5,8,9,13–15,27]

Removal of the biofilm using the crystal violet assay. Bacteria with a density of 1.3×10^6 cfu mL^{-1} were inoculated into LB agar broth medium for *P. aeruginosa* or tryptic soy broth for *S. aureus* (total volume = 1500 μL) in test tubes and cultured for 20 h at 37 °C. Afterwards, the content of each test tube was carefully removed, the tubes were washed with 1 mL of 0.9% saline dilution and 2 mL of broth was added. The negative control contained only broth. Then, the bacteria were incubated with **AGGLY**, **AGU**, pHEMA, **pHEMA@AGGLY-2**, **pHEMA@AGU-2** and **pHEMA@AGSAL-2** discs for 20 h, at 37 °C. The content of each tube was then poured and was washed three times with 1 mL of methanol and 2 mL of 0.9% saline and left to dry. Then, the tubes were stained for 15 min with a crystal violet solution (0.1% w/v). Excess stain was rinsed off with 1 mL of methanol and 2 mL of 0.9% saline solution and then with 3 mL of 0.9% saline solution. The tubes were left to dry for 24 h and the bound crystal violet was released by adding 30% glacial acetic acid. The optical density of the solution yielded was then measured at 550 nm, to give the biofilm biomass.[5,8,9,13–15,27]

Sulforhodamine B assay. Initially, the HCECs were seeded in a 24-well plate at a density of 7.5×10^4 cells and after 24 hours of cell incubation, **AGGLY**, **AGU**, **AGSAL**, and the discs of pHEMA, **pHEMA@AGGLY-2**, **pHEMA@AGU-2** and **pHEMA@AGSAL-2** were added into the wells. After 24 hours of incubation of the HCECs with the discs, the discs were removed and the culture medium was aspirated and the cells were fixed with 300 μL of 10% cold trichloroacetic acid (TCA). The plate was left for 30 min at 4 °C, washed five times with deionized water, and left to dry at room temperature for at least 24 h. Subsequently, 300 μL of 0.4% (w/v) sulforhodamine B (SRB) (Sigma) in 1% acetic acid solution was added to each well and left at room temperature for 20 min. SRB was removed, and the plate was washed five times with 1% acetic acid before air drying. Bound SRB was solubilised with 1 mL of 10 mM un-buffered Tris-base solution. Absorbance was read on a 24-well plate reader at 540 nm.[5,8,9,13–15,27]

Evaluation of *in vitro* genotoxicity with the micronucleus assay. The evaluation of the genotoxicity of pHEMA, **pHEMA@AGGLY-2**, **pHEMA@AGU-2** and **pHEMA@AGSAL-2** was performed following the protocol reported elsewhere.[5,8,9,13–15,27] HCECs were seeded (7×10^4 cells per well) in glass cover slips which were afterwards placed in six-well plates, with 3 mL of cell culture medium and incubated for 24 h. Then the HCECs were exposed to the discs for a period of 48 h. After the exposure to the biomaterials, the cover slips were washed three times with PBS and once with a hypotonic solution (75 mM KCl) for 10 min at room temperature. The hypotonized cells were fixed by at least three changes of 1/3 acetic acid/methanol solution. The cover slips were also washed with cold methanol containing 1% acetic acid. The cover slips were then stained with acridine orange (50 μg mL^{-1}) for 15 min at 37 °C. After that the cover slips were rinsed three times with PBS to remove any excess acridine orange. The number of micronucleated cells per 1000 cells was determined.

Evaluation of toxicity with the brine shrimp assay. The brine shrimp assay was performed by a method previously described.[32] An aliquot (0.1 mL) containing about 6 to 10 nauplii was introduced to each well of a 24-well plate and one disc of pHEMA, **pHEMA@AGGLY-2**, **pHEMA@AGU-2** and **pHEMA@AGSAL-2** was added into each well. The final volume of each well is 1 mL with NaCl 0.9%. The brine shrimps were observed at the interval time of 24 hours, using a stereoscope. The larvae are considered dead if they do not show any internal or external movement in 10 seconds of observation. Each experiment was repeated three times.

Evaluation of *in vivo* genotoxicity with the *Allium cepa* test. The *in vivo* genotoxicity was assessed following the already known method.[31] Small bulbs (~1.0–1.5 cm in diameter) of *Allium cepa* were purchased from the local market. Bulbs of *Allium cepa* were placed in test tubes (16 ml) which were filled with water and placed in the incubator at 25 °C, 50–60% humidity and 12 h day lighting/12 h dark for 48 h. The discs of pHEMA, **pHEMA@AGGLY-2**, **pHEMA@AGU-2** and **pHEMA@AGSAL-2** were added into the test tubes to incubate the bulbs for 48 h. The roots growing in double distilled water were used as control. In order to evaluate the rate of the cellular division, the microscopic parameter of the mitotic index was determined. All categories were analyzed by counting 1800 cells per concentration (300 cells per slide, a total of six slides).

Conflicts of interest

There are no conflicts to declare by the authors.

Acknowledgements

This research has been co-financed by the European Union and Greek national funds through the Operational Program Competitiveness, Entrepreneurship and Innovation, under the call RESEARCH – CREATE – INNOVATE (project code: T1EDK-02990). Professor T. Vaimakis is acknowledged for the TG-DTA/DSC measurements. The COST Action CA15114 "Anti-Microbial Coating Innovations to prevent infectious diseases (AMICI)" is acknowledged for the stimulating discussions.

This work was carried out in fulfilment of the requirements for the Master thesis of Ms M. K. according to the curriculum of the International Graduate Program in "Biological Inorganic Chemistry", which operates at the University of Ioannina within the collaboration of the Departments of Chemistry of the Universities of Ioannina, Athens, Thessaloniki, Patras, Crete and the Department of Chemistry of the University of Cyprus (http://bic.chem.uoi.gr/BIC-En/index-en.html) under the supervision of Prof. S. K. H.

References

1 A. Xiao, C. Dhand, C. M. Leung, R. W. Beuerman, S. Ramakrishna and R. Lakshminarayanan, Strategies to design antimicrobial contact lenses and contact lens cases, *J. Mater. Chem. B*, 2018, **6**, 2171–2186.

2 C. Dhand, C. Y. Ong, N. Dwivedi, J. Varadarajan, M. H. Periayah, E. J. Lim, V. Mayandi, E. T. Leng Goh, R. P. Najjar, L. W. Chan, R. W. Beuerman, L. L. Foo, X. J. Loh and R. Lakshminarayanan, Mussel-Inspired Durable Antimicrobial Contact Lenses: The Role of Covalent and Noncovalent Attachment of Antimicrobials, ACS Biomater, *Sci. Eng.*, 2020, **6**, 3162–3173.

3 D. Kharaghani, D. Dutta, P. Gitigard, Y. Tamada, A. Katagiri, D.-N. Phan, M. D. P. Willcox and I. Soo Kim, Development of antibacterial contact lenses containing metallic nanoparticles, *Polym. Test.*, 2019, **79**, 106034.

4 S. Ahmad Khan and C.-S. Lee, Recent progress and strategies to develop antimicrobial contact lenses and lens cases for different types of microbial keratitis, *Acta Biomater.*, 2020, **113**, 101–118.

5 A. K. Rossos, C. N. Banti, A. Kalampounias, C. Papachristodoulou, K. Kordatos, P. Zoumpoulakis, T. Mavromoustakos, N. Kourkoumelis and S. K. Hadjikakou, pHEMA@AGMNA-1: A novel material for the development of antibacterial contact lens, *Mater. Sci. Eng., C*, 2020, **111**, 110770.

6 https://www.cdc.gov/contactlenses/fast-facts.html.

7 D. Dutta and M. D. P. Willcox, Antimicrobial Contact Lenses and Lens Cases, *Eye Contact Lens*, 2014, **40**, 312–324.

8 A. Meretoudi, C. N. Banti, P. K. Raptis, C. Papachristodoulou, N. Kourkoumelis, A. A. Ikiades, P. Zoumpoulakis, T. Mavromoustakos and S. K. Hadjikakou, Silver Nanoparticles from Oregano Leaves' Extracts as Antimicrobial Components for Non-Infected Hydrogel Contact Lenses, *Int. J. Mol. Sci.*, 2021, **22**, 3539.

9 I. Milionis, C. N. Banti, I. Sainis, C. P. Raptopoulou, V. Psycharis, N. Kourkoumelis and S. K. Hadjikakou, Silver ciprofloxacin (CIPAG): a successful combination of chemically modified antibiotic in inorganic–organic hybrid, *J. Biol. Inorg. Chem.*, 2018, **23**, 705–723.

10 V. A. Karetsi, C. N. Banti, N. Kourkoumelis, C. Papachristodoulou, C. D. Stalikas, C. P. Raptopoulou, V. Psycharis, P. Zoumpoulakis, T. Mavromoustakos, I. Sainis and S. K. Hadjikakou, An Efficient Disinfectant, Composite Material {SLS@[Zn_3($CitH)_2$]} as Ingredient for Development of Sterilized and Non Infectious Contact Lens, *Antibiotics*, 2019, **8**, 213.

11 L. Kyros, C. N. Banti, N. Kourkoumelis, M. Kubicki, I. Sainis and S. K. Hadjikakou, Synthesis, characterization, and binding properties towards CT-DNA and lipoxygenase of mixed-ligand silver(I) complexes with 2-mercaptothiazole and its derivatives and triphenylphosphine, *J. Biol. Inorg. Chem.*, 2014, **19**, 449–464.

12 I. Sainis, C. N. Banti, A. M. Owczarzak, L. Kyros, N. Kourkoumelis, M. Kubicki and S. K. Hadjikakou, New antibacterial, non-genotoxic materials, derived from the functionalization of the anti-thyroid drug methimazole with silver ions, *J. Inorg. Biochem.*, 2016, **160**, 114–124.

13 M.-E. K. Stathopoulou, C. N. Banti, N. Kourkoumelis, A. G. Hatzidimitriou, A. G. Kalampounias and S. K. Hadjikakou, Silver complex of salicylic acid and its hydrogel-cream in wound healing chemotherapy, *J. Inorg. Biochem.*, 2018, **181**, 41–55.

14 M. P. Chrysouli, C. N. Banti, I. Milionis, D. Koumasi, C. P. Raptopoulou, V. Psycharis, I. Sainis and S. K. Hadjikakou, A water-soluble silver(I) formulation as an effective disinfectant of contact lenses cases, *Mater. Sci. Eng. C*, 2018, **93**, 902–910.

15 I. Ketikidis, C. N. Banti, N. Kourkoumelis, C. G. Tsiafoulis, C. Papachristodoulou, A. G. Kalampounias and S. K. Hadjikakou, Conjugation of Penicillin-G with Silver(I) Ions Expands Its Antimicrobial Activity against Gram negative Bacteria, *Antibiotics*, 2020, **9**, 25.

16 P. J. Cox, P. Aslanidis, P. Karagiannidis and S. Hadjikakou, Silver(I) complexes with heterocyclic thiones and tertiary phosphines as ligands. Part 4. Dinuclear complexes of silver(I) bromide: the crystal structure of bis[bromo-(pyrimidine-2-thione)(triphenylphosphine)silver(I), *Inorg. Chim. Acta*, 2000, **310**, 268–272.

17 S. Zartilas, N. Kourkoumelis, S. K. Hadjikakou, N. Hadjiliadis, P. Zachariadis, M. Kubicki, A. Y. Denisov and I. S. Butler, A new silver(I) aggregate having an octagonal Ag4S4 core where μ3-S bonding interactions lead to a nano-tube assembly which exhibits quasi-aromaticity, *Eur J. Inorg. Chem.*, 2007, 1219–1224.

18 S. K. Hadjikakou, I. I. Ozturk, M. N. Xanthopoulou, P. C. Zachariadis, S. Zartilas and N. Hadjiliadis, Synthesis, Structural Characterization and Biological Study of New Organotin(IV), Silver(I) and Antimony(III) Complexes with Thioamides, *J. Inorg. Biochem.*, 2008, **102**, 1007–1015.

19 S. Zartilas, S. K. Hadjikakou, N. Hadjiliadis, N. Kourkoumelis, L. Kyros, M. Kubicki, M. Baril, I. S. Butler, S. Karkabounas and J. Balzarini, Tetrameric 1:1 and monomeric 1:3 complexes of silver(I) halides with tri(p-tolyl)-phosphine: A structural and biological study, *Inorg. Chim. Acta*, 2009, **362**, 1003–1010.

20 P. C. Zachariadis, S. K. Hadjikakou, N. Hadjiliadis, A. Michaelides, S. Skoulika, Y. Ming and Y. Xiaolin,

Synthesis, study and structural characterisation of a new water soluble hexanuclear silver(I) cluster with the 2-mercapto-nicotinic acid with possible antiviral activity, *Inorg. Chim. Acta*, 2003, **343**, 361–365.

21 P. C. Zachariadis, S. K. Hadjikakou, N. Hadjiliadis, A. Michaelides, S. Skoulika, J. Balzarini and E. D. Clercq, Synthesis, characterization and in vitro study of the cytostatic and antiviral activity of new polymeric silver(I) complexes with ribbon structures, derived from the conjugated heterocyclic thioamide 2-mercapto-3,4,5,6-tetrahydro-pyrimidine, *Eur. J. Inorg. Chem.*, 2004, 1420–1426.

22 C. N. Banti, C. P. Raptopoulou, V. Psycharis and S. K. Hadjikakou, Novel silver glycinate conjugate with 3D polymeric intermolecular self-assembly architecture; an antiproliferative agent which induces apoptosis on human breast cancer cells, *J. Inorg. Biochem.*, 2021, **216**, 111351.

23 M. Poyraz, C. N. Banti, N. Kourkoumelis, V. Dokorou, M. J. Manos, M. Simčič, S. Golič-Grdadolnik, T. Mavromoustakos, A. D. Giannoulis, I. I. Verginadis, K. Charalabopoulos and S. K. Hadjikakou, Synthesis, structural characterization and biological studies of novel mixed ligand Ag(I) complexes with triphenylphosphine and aspirin or salicylic acid, *Inorg. Chim. Acta*, 2011, **375**, 114–121.

24 D. S. Sagatys, R. C. Bott, G. Smith, K. A. Byriel and C. H. L. Kennard, The preparation and crystal structure of a polymeric (1:1)-silver nitrate urea complex, $[(AgNO_3)_2(CH_4N_2O)_2]_n$, *Polyhedron*, 1992, **11**, 49–52.

25 F. J. Carmona, G. D. Sasso, G. B. Ramírez-Rodríguez, Y. Pii, J. M. Delgado-López, A. Guagliardi and N. Masciocchi, Urea-functionalized amorphous calcium phosphate nanofertilizers: optimizing the synthetic strategy towards environmental sustainability and manufacturing costs, *Sci. Rep.*, 2021, **11**, 3419.

26 M. A. C. de Oliveira, P. P. M. Pico, W. da Silva Freitas, A. D'Epifanio and B. Mecheri, Iron-Based Electrocatalysts for Energy Conversion: Effect of Ball Milling on Oxygen Reduction Activity, *Appl. Sci.*, 2020, **10**, 5278.

27 M. P. Chrysouli, C. N. Banti, N. Kourkoumelis, E. E. Moushi, A. J. Tasiopoulos, A. Douvalis, C. Papachristodoulou, A. G. Hatzidimitriou, T. Bakas and S. K. Hadjikakou, Ciprofloxacin conjugated to diphenyltin (IV): a novel formulation with enhanced antimicrobial activity, *Dalton Trans.*, 2020, **49**, 11522–11535.

28 M. Elder, F. Stapleton, E. Evans and J. K. G. Dart, Biofilm-related infections in ophthalmology, *Eye*, 1995, **9**, 102–109.

29 H. Hintzsche, G. Montag and H. Stopper, Induction of micronuclei by four cytostatic compounds in human hematopoietic stem cells and human lymphoblastoid TK6 cells, *Sci. Rep.*, 2018, **8**, 3371.

30 M. Fenech, Cytokinesis-block micronucleus cytome assay, *Nat. Protoc.*, 2007, **2**, 1084–1104.

31 C. N. Banti and S. K. Hadjikakou, Evaluation of Genotoxicity by Micronucleus Assay in vitro and by Allium cepa Test in vivo, *Bio-Protoc.*, 2019, **9**, e3311.

32 C. N. Banti and S. K. Hadjikakou, Evaluation of Toxicity with Brine Shrimp Assay, *Bio-Protoc.*, 2021, **11**, e3895.

33 A. F. Trompeta, I. Preiss, F. Ben-Ami, Y. Benayahu and C. A. Charitidis, Toxicity testing of MWCNTs to aquatic organisms, *RSC Adv.*, 2019, **9**, 36707–36716.

34 M. Ates, J. Daniels, Z. Arslan, I. O. Farah and H. F. Rivera, Comparative evaluation of impact of Zn and ZnO nanoparticles on brine shrimp (Artemia salina) larvae: effects of particle size and solubility on toxicity, *Environ. Sci.: Processes Impacts*, 2013, 15225–15233.

35 B. Zhu, S. Zhu, J. Li, X. Hui and G.-X. Wang, The developmental toxicity, bioaccumulation and distribution of oxidized single walled carbon nanotubes in Artemia salina, *Toxicol. Res.*, 2018, 7897–7906.

36 C. N. Banti, N. Kourkoumelis, A. G. Hatzidimitriou, I. Antoniadou, A. Dimou, M. Rallis, A. Hoffmann, M. Schmidtke, K. McGuire, D. Busath, A. Kolocouris and S. K. Hadjikakou, Amantadine copper(II) chloride conjugate with possible implementation in influenza virus inhibition, *Polyhedron*, 2020, **185**, 114590.

37 M. Ç. Akgündüz, K. Çavuşoğlu and E. Yalçın, The Potential Risk Assessment of Phenoxyethanol with a Versatile Model System, *Sci. Rep.*, 2020, **10**, 1209.

38 S. A. S. Mercado and J. D. Q. Caleño, Cytotoxic evaluation of glyphosate, using Allium cepa L. as bioindicator, *Sci. Total Environ.*, 2020, **700**, 134452.

39 Rigaku/MSC, *CrystalClear*, Rigaku/MSC Inc., The Woodlands, Texas, USA, 2005.

40 G. M. Sheldrick, A short history of SHELX, *Acta Crystallogr., Sect. A: Found. Crystallogr.*, 2008, **64**, 112–122.

41 G. M. Sheldrick, Crystal structure refinement with SHELXL, *Acta Crystallogr., Sect. C: Struct. Chem.*, 2015, **71**, 3–8.

42 *DIAMOND-Crystal and Molecular Structure Visualization, Ver. 3.2, Crystal Impact*, Rathausgasse 30, 53111, Bonn, Germany.